RSC Advances

ROYAL SOCIETY OF CHEMISTRY

www.rsc.org/advances

RSC Advances

ARTICLE

High-field Antiferroelectric-like Behavior in Uniaxially Stretched Poly(vinylidene fluoride-trifluoroethylene-chlorotrifluoroethylene) -*grafted*-poly(methyl methacrylate) Films with High Energy Density

Received 00th January 20xx,
Accepted 00th January 20xx

DOI: 10.1039/x0xx00000x

www.rsc.org/

Honghong Gong,[a] Bei Miao,[a] Xiao Zhang,[b] Junyong Lu*[b] and Zhicheng Zhang*[a]

In an effort to achieve antiferroelectric-like behavior and high U_e under high electric field, a series of poly(methyl methacrylate) (PMMA) grafted P(VDF-TrFE-CTFE) with increased PMMA content were synthesized *via* an atom transfer radical polymerization process. All the grafted copolymer films were prepared by a solution-casting process followed by uniaxially stretched with varied extension ratios. The dependence of crystalline, ferroelectric, dielectric and energy storage properties on both orientation ratio and PMMA content was systematically discussed. Beside of the orientation of the polymer chains in amorphous phase together with the alignment of crystalline and ferroelectric grains, uniaxially drawing the films leads to the improved both the content and size of crystalline and ferroelectric phases. Thanks to the strong confinement of rigid PMMA and the alignment induced high breakdown strength, the antiferroelectric-like behavior could be retained up to 675 MV/m with a discharged energy density of 23.3 J/cm^3 in the copolymer bearing 24 wt% PMMA with an extension ratio of 300%. These results may help to deeply understand the ferroelectric transition mechanism of PVDF based ferroelectric polymers and provide a promising strategy for the design of polymers with high energy storage capability.

1. Introuction

Driven by the requirements of green energy for the electronic and electrical industries, dielectric polymer films with high energy storage capability (U_e) and low energy loss (U_l) has attracted a great deal of attention during past decades.[1-4] Among the currently utilized dielectric polymers, BOPP is the state-of-the-art metalized polymeric film for capacitors because of its high electric strength (E_b > 700 MV/m) and low dielectric loss (*tan*δ < 0.0002@1 kHz). Limited by its low dielectric constant (ε_r) about 2.2, U_e of BOPP relies on the high E_b mostly and is rather low even under very high electric field (c.a. 4.88 J/cm^3 at 700 MV/m).[5-7] By introducing polar groups (c.a. -OH and -NH_2) onto the polymer chains, the dielectric constant of PP could be increased to 4-6, and the stored energy density could be enhanced up to 8 J/cm^3 at 600 MV/m field as well.[8-10]

Among the known commercial polymers, poly(vinylidene fluoride) (PVDF) based fluoropolymers have attracted continuously increasing interests as dielectric materials for their relatively high ε_r of 10-12 beside of their well-known excellent ferro- and piezo-electric properties.[11-16] However, PVDF based normal ferroelectric polymers render a rather small U_e owing to the large remnant polarization (P_r) and low saturation electric field (E_s). To release the energy stored, many efforts have been devoted to modify PVDF and its copolymers physically and chemically, and they have been successfully turned from normal ferroelectrics into relaxed ferroelectrics.[13, 17-28] However, due to their ferroelectric relaxation nature, the charge and discharge curves on displacement-electric field (D-E) hysteresis loops do not match very well and relatively large hysteresis together with high U_l (about 40%) are observed.

To confine the ferroelectric relaxation by weakening the coupling among adjacent ferroelectric domains, low polar polystyrene (PS) has been introduced in P(VDF-CTFE) and P(VDF-TrFE-CTFE) as side chains to form micro-insulator layers surrounding the ferroelectric domains. Due to the low polarity of the PS-rich layer at the amorphous-crystalline interface, the compensation polarization is substantially decreased resulting in a novel confined ferroelectric behavior in the grafted copolymers. Rather low dielectric loss (*tan*δ of 0.006@1 kHz) and U_l of 17.5%@550 MV/m are detected in P(VDF-CTFE)-*g*-PS (34 wt%) copolymers, although U_e is reduced from 9.2 to 4.8 J/cm^3 at 400 MV/m as well.[29] Most interestingly, drawing P(VDF-TrFE-CTFE)-*g*-PS bearing 14 wt% of PS segment uniaxially results into the ferroelectric transition from linear dielectrics to ferroelectrics with a double hysteresis loops (DHLs), which is closely dependent on the extension ratio. Comparing with the DHLs observed in PVDF based normal ferroelectrics under low electric field in a very narrow range and within limited polarizing

[a] Department of Applied Chemistry, MOE Key Laboratory for Nonequilibrium Synthesis and Modulation of Condensed Matter, School of Science, Xi'an Jiaotong University, Xi'an, P. R. China, 710049, Email: zhichengzhang@mail.xjtu.edu.cn.
[b] National Key Laboratory of Science and Technology on Vessel Integrated Power System, Naval University of Engineering, Wuhan, P. R. China, 430034, Email: jylu@xinhuanet.com.

circles, DHLs are found to be well maintained under relatively high electric field in the stretched P(VDF-TrFE-CTFE)-*g*-PS films. However, when the extension ratio is 450%, the U_e is obtained as only 2.5 J/cm^3@150 MV/m together with U_l approximate 30% in the grafted polymer films mainly due to the quickly vanishing of DHL behavior under elevated electric field.[30,31] Therefore, fabricating polymeric films with antiferroelectric-like behavior under high electric field together with high breakdown strength should be a desirable way to achieve high U_e in metalized film capacitors.

Instead of low polar PS, different poly(methacrylic ester)s (PXMAs) were grafted onto P(VDF-TrFE-CTFE) and the introduction of PXMA with excellent compatibility with the main chains could effectively impede the crystallization of P(VDF-TrFE-CTFE). The D-E hysteresis behaviors of P(VDF-TrFE-CTFE) were finely tuned from typical ferroelectric to either anti-ferroelectric or linear dielectric by facilely grafting the required types and amount of XMA monomers onto it. The outstanding confining and decoupling effects of PXMA side chains on the disorientation of the high polar crystal domains and the transition from normal ferroelectric to anti-ferroelectric or linear dielectric are responsible for its significantly decreased U_l, well maintained U_e and the greatly improved E_s. A low U_l of 16.6% and relatively high U_e of 19.3 J/cm^3 under electric field of 675 MV/m was achieved in P(VDF-TrFE-CTFE)-*g*-PEMA copolymer.[32] Among all the investigated three types of PXMA, poly(methyl methacrylate) (PMMA) exhibits the strongest confinement onto the ferroelectric performance of P(VDF-TrFE) for its highest polarity, modulus at ambient temperature and glass transition temperature (T_g).

In an effort to improve the breakdown strength and retain the anti-ferroelectric behavior under high electric field, in this work, uniaxial stretching has been conducted onto a family of solution cast P(VDF-TrFE-CTFE)-*g*-PMMA films bearing different PMMA content. The dependence of the crystalline, dielectric and ferroelectric properties of the films with varied PMMA content on the extension ratio has been carefully investigated. Thanks to the strong confinement of PMMA side chains and orientation induced ferroelectric phase transition, DHL behavior of P(VDF-TrFE-CTFE)-*g*-PMMA with 24 wt% of PMMA and an extension ratio of 300% could be well maintained up to 675 MV/m and the highest U_e is obtained as 23.3 J/cm^3. Meanwhile, the uniaxial stretching is also found be responsible for the significantly improved E_b comparing with the as-casted films, thus the significantly increased U_e at E_b.

2. Experimental

2.1 Materials

P(VDF-CTFE) samples (with 20 mol% CTFE) were purchased from China Bluestar Chengrand Chemical Co. Ltd. Methyl methacrylate (MMA) (Aladdin, 99%) were washed with 5 wt% NaOH solution and distilled under reduced pressure from CaH_2 to remove the inhibitor before used. Tetrahydrofuran (THF, Tianjin Reagents Co. Ltd, AR grade) was dried and distilled from sodium/benzophenone. CuCl (Sinopharm Reagents Co. Ltd, 97%), Cu powder (Sinopharm Reagents Co. Ltd, 75 μm, 99%), 2, 2-bipyridine (BPy, Alfa Aesar, 99%), *N*-methylpyrrolidinone (NMP, Tianjin Reagents Co. Ltd, AR grade), and *N*, *N*-dimethylformamide (DMF, Tianjin Reagents Co. Ltd AR grade) were used as received without further purification.

2.2 Synthesis of P(VDF-TrFE-CTFE)-*g*-PMMA *via* an ARGET-ATRP Process

The P(VDF-TrFE-CTFE)(80/18/2) was obtained with an hydrogenation of P(VDF-CTFE)(80/20) following the procedure as described in our previous work.[33] The P(VDF-TrFE-CTFE)-*g*-PMMA graft copolymers were synthesized by typical atom transfer radical polymerization (ARGET-ATRP) from P(VDF-TrFE-CTFE)(80/18/2) precursor terpolymer and using Cu as reductive agent as shown in Scheme 1. A 250 mL Schlenk flask equipped with magnetic stirring bar was charged with 6.0 g of P(VDF-TrFE-CTFE) and degassed for three times with dry nitrogen-vacuum cycles. 150 ml of NMP was purged with dry nitrogen for about 1 h and transferred into the Schlenk flask by a nitrogen-protected syringe. After the polymer was well dissolved, 1.008 g (6.4 mmol) of 2, 2-bipyridine, 0.318 g (3.2 mmol) of CuCl, and 0.204 g (3.2 mmol) of Cu and 8 ml of MMA were added. The polymerization was carried out at 100°C, and samples with varied grafting content were taken at regular time intervals. After re-dissolved in DMF and precipitated in water for three times to remove the catalyst residual, the crude product was washed with chloroform for 3 times to remove the homopolymers completely. The purified grafting copolymer was dried at 60°C under reduced pressure for 3 days.

Successful grafting of PMMA side chains from Cl sites in P(VDF-TrFE-CTFE) was characterized with ^{1}H NMR as shown in Scheme 1. Comparing with P(VDF-CTFE), new signals emerging at 5.3-5.8 ppm were assigned to the protons on TrFE (–CF_2C***F***–) converted from CTFE in P(VDF-CTFE). After grafted reaction, new signal at 3.5-3.7 is assigned to the protons on –OC***H***$_3$ of PMMA. The proton signals on VDF adjacent to CTFE (–CF_2–C***H***$_2$–CFCl–CF_2–) at 3.4-3.6 ppm vanish gradually as PMMA units are grafted. The chemical composition and the weight content of PMMA of the graft copolymer could be facilely calculated from ^{1}H NMR and the method had been reported in our previous work.[32]

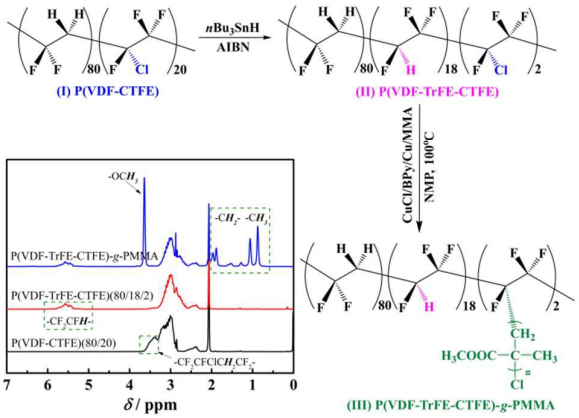

Scheme 1 Synthesis of P(VDF-TrFE-CTFE)-*g*-PMMA graft copolymer and ^{1}H NMR spectra of P(VDF-CTFE), P(VDF-TrFE-CTFE) and P(VDF-TrFE-CTFE)-*g*-PMMA.

2.3 Films Fabrication and Processing

All the graft copolymer films with a thickness of around 20 μm were prepared by cast the copolymer solution (about 3 wt% in DMF) onto glass plates at 70°C. After the solvent was evaporated completely, the films together with the plates were kept at 200°C for 4 h followed by immediately quenching in an ice-water bath. Then, the solution-casting films were uniaxially stretched at 100°C to different extension ratios at a speed of 10 mm/min using a home-built stretching apparatus. After stretching, the films were further annealed under tension at 100°C for 3 mins to release internal stresses before taken out quickly. The final thickness of stretched films is around 15 μm.

Films of the graft copolymers with different PMMA contents and extension ratios were named as follows. The film "10-100" denoted the nonstretched P(VDF-TrFE-CTFE)-*g*-PMMA(10 wt%) (100%), where number 10 refers to the weight content of PMMA (10 wt%) and number 100 indicates the extension ratio is 100% (nonstretched). Thus, "24-200" is for the sample containing 24 wt% PMMA with a stretching ratio of 200% as listed in Table 1.

2.4 Instruments and Characterization

^{1}H NMR spectra was recorded on a Bruker spectrometer (400 MHz, Advance III). X-ray diffraction (XRD) analysis was conducted on a Rigaku D/MAX-2400 (Rigaku Industrial Corp, Japan). The wavelength of the X-ray was 1.542 Å (Cu Kα radiation, 40 kV and 100 mA), and the scanning rate was 4°/min. Fourier transform infrared (FTIR) spectroscopy of the films was obtained on a Tensor 27 (Bruker, Germany) with a resolution of 1-0.4 cm^{-1} in transmission mode. Differential scanning calorimetric (DSC) analysis was conducted on a Netzsch DSC 200 PC (Netzsch, Germany) in a nitrogen atmosphere at a scanning rate of 10°C/min. SEM images were observed by JSM-6700F field emission scanning electron microscopy (SEM) instrument (JEOL, Ltd. Japan) after coated with gold. The dielectric properties were measured in a frequency range from 100 Hz to 1 MHz at 1 V using a HP (4284A) precision impedance analyzer. The electric D-E hysteresis loops at room temperature were determined on a Premiere II ferroelectric tester from Radiant Technologies, Inc., where AC electric fields ranging from 50-700 MV/m were applied onto polymer films with a triangular waveform at a frequency of 10 Hz. Gold electrodes (thickness 80 nm) were sputtered on both surfaces of the polymer films with a JEOL JFC-1600 auto fine coater (Japan). The breakdown electric field for all the sample films was determined by the breakdown voltage tester (Beijing Beiguangjingyi Instrument Equipment Co., LTD) and the electric field applied rate of 1 kV/min. The diameter of the cylindrical electrode was 10 mm. The leakage current was obtained as less than 10 mA until the film was broken down.

3. Results and discussion

3.1 Orientation induced crystalline and F-P phase transition

For the PVDF based fluoropolymers, uniaxial stretching may lead to the crystalline phase and ferro- to para-electric phase transition as well.[34-41] To investigate how the uniaxial orientation influences the crystalline and F-P phase transition of the PMMA grafted P(VDF-TrFE-CTFE) copolymers, the films containing varied PMMA content from 10 wt% to 24 wt% and drawn in different ratios up to 400% were carefully characterized. First of all, these films were examined with XRD spectra as shown in Fig. 1. For the nonstretched samples (extension ratio = 100%), only typical β-phase P(VDF-TrFE) crystals were observed as evidenced by the (110/200) reflection peak at 2θ = 19.4°, which is corresponding to the *all-trans* chain conformation stabilized by the high content of TrFE units (18 mol%). Meanwhile, the introduction of PMMA segments is favorable for the formation of high polar γ- or β-phase in PVDF.[16] That may address for the results observed from XRD that sole β-phase P(VDF-TrFE) is detected in all the as-casted samples. That could be further confirmed by the FTIR spectra in Fig. 2, where typical β-form absorption bands were observed at 842, 505 and 470 cm^{-1}, respectively. Moreover, the single melting peak around 120°C in DSC curves shown in Fig. 3 strongly suggests the pure β-form crystals as well.[42] Meanwhile, the increasing of PMMA content would lead to the decreased crystallinity as well as the reduced crystal size, which could be confirmed by the vanished peak at 19.4° on XRD and the reduced melting peak at 120-130°C on DSC in the as-casted films with PMMA content increasing from 10 wt% to 24 wt% gradually.

Uniaxial stretching below the melting temperature of PVDF is widely utilized to transfer the low polar α or γ crystals into high polar β-PVDF for high ferro- and piezo-electricity.[34-38] Only β-phase is detected in present PMMA-grafted polymers and the uniaxial stretching is not necessary to realize the crystal phase transition. However, the stretching does lead to the significantly improved crystallinity. Comparing with the as-casted films, the stretched samples possess significantly sharpened reflection peak at 2θ = 19.4° in XRD spectra and reduced dispersive peak at about 17° attributed to the amorphous structure. That means the orientation may lead to the crystallization of P(VDF-TrFE) main chain in amorphous phase along the drawing direction, which may be confirmed by the sharpened absorption peaks corresponding to β-PVDF in FTIR results as well. To quantificationally characterize the phase transition happened during the stretching, the apparent crystallite size along (110/200) [$D_{(110/200)\beta}$] was calculated using the Scherrer equation: $D_{hkl} = (K\cdot\lambda)/(B_{hkl}\cdot\cos\theta)$, where D_{hkl} is the average crystallite size along the (hkl) direction, K is the shape factor (a value of 0.94 is used in this case), λ is the wavelength, and B_{hkl} is the full width at half-maximum for the (hkl) diffraction. As shown in Table 1, after uniaxially stretched at 100°C, the crystalline size of lamellae is significantly increased, especially for the samples containing more PMMA side chains. For example, D_{hkl} of 21-100 is improved from 3.9 nm to 5.9 nm of 21-300, and D_{hkl} of 24-100 is improved from 3.0 nm to 5.6 nm of 24-300. In addition, the crystallinity of all the samples was evaluated with DSC by $\chi_c = H_f/(H_f^0\cdot\omega)$, where H_f^0 = 104.7 J/g is the enthalpy of PVDF with 100% crystallinity, ω is the weight percent of the P(VDF-TrFE-CTFE) in the graft copolymer. As listed in Table 1, both the crystallinity and melting temperature of samples is more or less increased after stretched. That means the uniaxial orientation is favorable of the increasing of crystallinity and crystal grain size. The reduction in amorphous phase and increase in crystal phase observed in XRD results could clearly demonstrate that the improved crystalline

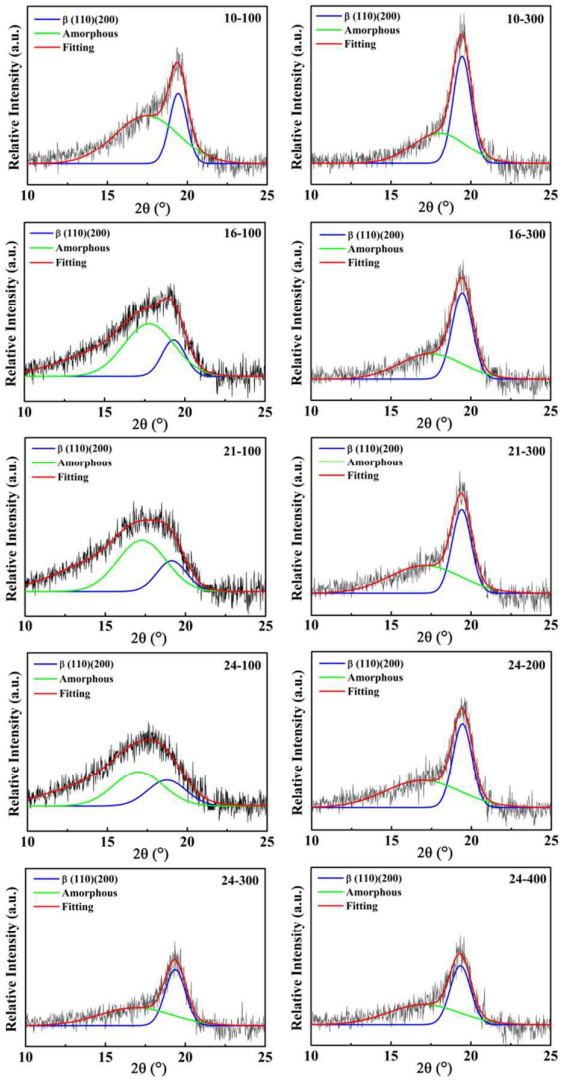

Fig. 1 XRD spectra of as-casted and after uniaxial stretched P(VDF-TrFE-CTFE)-*g*-PMMA films containing various content of PMMA.

properties are mostly originating from the orientation induced recrystallization of polymer chains in amorphous phase.

As presented in Fig. 3, comparing to the as-casted samples, the stretched films possess about 2-4°C elevated F-P temperature and the sharpened peak. The content of ferroelectric phase could be estimated with the enthalpy (ΔH_C) of F-P transition peak on DSC. As listed in Table 1, the stretched samples show improved ΔH_C as well as the Curie temperature (T_C), which means both the size and content of the ferroelectric phase are improved induced by the orientation. It has been known that the P(VDF-TrFE) ferroelectrics possess the typical order-disorder character change associated with ferro- to para- electric transition. The ferroelectric phase basically consists of regular all-*trans* polymer chains packed in parallel or β-form crystals. Meanwhile, a certain amount of disorder comprising some defects would be generated for the quenching process from

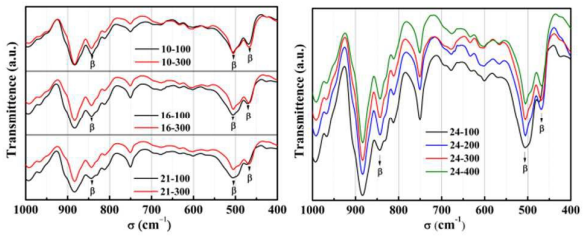

Fig. 2 FTIR spectra of P(VDF-TrFE-CTFE)-*g*-PMMA films before and after uniaxial stretching.

high temperature.[15] As temperature approaches T_C, such disorder grows rapidly to divide all-*trans* regions into sub-domains, which may undergo large fluctuations as a result of the competition between the cooperative and entropy forces. In the paraelectric phase, both the size and the volume fraction of such sub-domains would be diminished with the increasing of temperature. The introduction of rigid amorphous PMMA chains may improve T_C by strengthening ferroelectric domain wall and reduced ΔH_C by decreasing the ferroelectric domain contents. Apparently, both the improved T_C and ΔH_C in all the stretched films mean the orientation facilitates more and large order structures and thus the ferroelectric domains. With the assistance of stretching uniaxially, both the size and the content of the ferroelectric domains are improved as indicated in Table 1. Apparently, the impedance effect of PMMA onto the formation of crystalline and ferroelectric phase in large scale is weakened by the stretching.

In general, uniaxially stretching the P(VDF-TrFE-CTFE)-*g*-PMMA films results in the improved crystallinity as well as the thickness of crystal grains but invisible change of crystal forms. Meanwhile, the F-P phase transition performance of the grafted copolymers has been enhanced as well characterized with both increased ΔH_C and T_C. Besides, stretching would lead to part of the pre-existing flat-on β crystals in as-casted films be pulled apart and orientated with their c-axes parallel (or the crystalline lamellae transverse) to the drawing direction, which has been well reported in literature.[27,43]

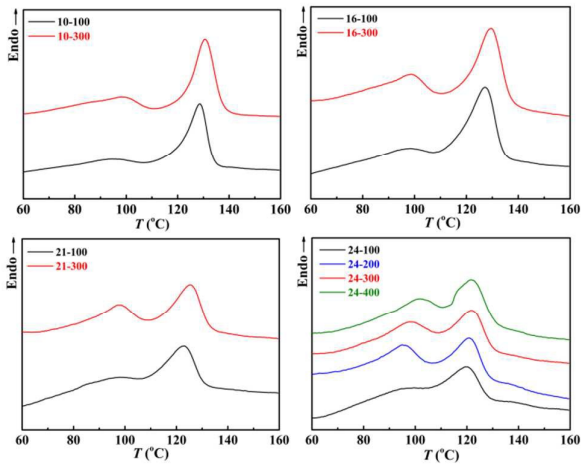

Fig. 3 DSC curves of P(VDF-TrFE-CTFE)-*g*-PMMA films before and after uniaxial stretching.

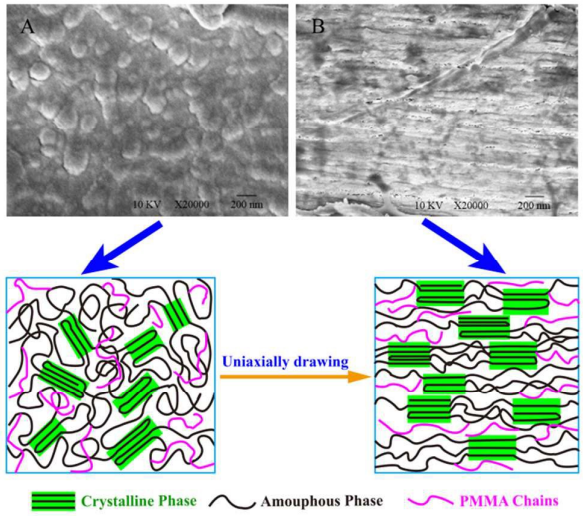

Fig. 4 SEM images of sections of P(VDF-TrFE-CTFE)-g-PMMA films (A, 21-100; B, 21-300) and scheme of lamellae orientation in the film before and after uniaxially stretched.

Most importantly, stretching would cause the orientation ofpolymer chain in amorphous phases as well as the ferroelectric domains. From the SEM images and the cartoon as show in the Fig. 4, the well-grown lamellae are usually aligned along the thickness direction of the films.

3.2 Dielectric Properties at Low Electric Field

The dielectric constant (ε_r) and dielectric loss ($tan\delta$) were measured as a function of frequency for all films under a low electric field (voltage = 1 V) as shown in Fig. S4. ε_r is slightly decreasing against the testing frequency for all P(VDF-TrFE-CTFE)-*g*-PMMA samples because of their ferroelectric and nonlinear in nature. Meanwhile, ε_r of nonstretched films is decreasing as a function of PMMA content. Besides, the sharply decreasing on ε_r curves at high frequency (10^5 ~ 10^6 Hz), corresponding to the so-called β-relaxation related to the micro-Brownian motion of non-crystalline chain segments and the molecular motion on the amorphous/crystalline interfaces, is turned into flat one as PMMA content increases. That could be attributed to the confinement effect from rigid PMMA chains in addition to the dilution effect of relatively low polarizability PMMA chains (ε_r ~ 3.5), which has been finely discussed previously.[32,33] Therefore, the immobilizing effect of rigid amorphous phase on the spatial rotation of dipoles in both amorphous and crystalline phases is responsible for the lowered ε_r. Correspondingly, the dielectric loss of the films is reduced as more PMMA side chains are grafted due to the depressed mobility of dipole moments as well as the β-relaxation.

Comparing with the as-casted films, uniaxial stretched samples exhibit significantly increased ε_r as indicated in Fig. S4. It has been well reported that the dielectric properties of PVDF and its copolymers are anisotropic with respect to different crystal orientations.[34-36] In the as-casted films, the ferroelectric domains are dispersed randomly in all the directions although the dipole moments of CF_2 in these domains are well aligned and densely packed together. Under low electric field, the contribution of these isotopically distributed ferroelectric domains to the dielectric constant shows no priority along the dielectric field than the other directions. However, the polymer chains both in crystal and amorphous phase of the stretched samples would be aligned along the drawing direction and perpendicular to the external field. As a result, the dipoles exhibit a priority in a plane parallel to the electric field depending on the stretching ratio. The orientation

Table 1 The crystalline data of P(VDF-TrFE-CTFE)-*g*-PMMA films.

Entry	Mole ratio[a]	PMMA / wt%[b]	*D* / nm[c]	T_C / °C[d]	ΔH_C / J·g^{-1}[d]	T_m / °C[d]	χ_c / %[d]
10-100	80/18/2/7.6	10	6.5	95.2	2.4	128.7	9.6
10-300	80/18/2/7.6	10	6.7	98.1	5.0	130.6	11.3
16-100	80/18/2/12.7	16	5.0	98.5	2.1	127.3	8.3
16-300	80/18/2/12.7	16	5.6	98.8	4.1	129.5	8.5
21-100	80/18/2/18.6	21	3.9	97.0	1.9	122.9	5.0
21-300	80/18/2/18.6	21	5.9	97.7	3.4	125.6	5.5
24-100	80/18/2/21.7	24	3.0	95.0	1.1	119.4	3.0
24-200	80/18/2/21.7	24	5.9	96.0	2.8	121.0	3.5
24-300	80/18/2/21.7	24	5.6	98.6	2.5	121.5	3.3
24-400	80/18/2/21.7	24	5.6	101.8	2.0	122.0	3.7

[a]The mole ratio of VDF/TrFE/CTFE/MMA determined by ^{1}H NMR. [b]The weight percentage of PMMA in P(VDF-TrFE-CTFE)-*g*-PMMA graft copolymers. [c]The apparent crystallite size along (110/200)[$D_{(110/200)\beta}$] calculated using the Scherrer equation. [d]Determined by DSC during the second heating process. ΔH_c is the heat enthalpy of the Curie transition for the copolymer.

polarizability of transverse crystals and aligned amorphous phase is enhanced, which contributes a lot to ε_r. Apparently, the alignment of dipole moments plays a crucial role in the improvement of ε_r besides of their polarity. The continuously improved dielectric constant from the sample 24-100 to 24-400 could further confirm the significant contribution of dipole orientation onto ε_r. That could be explained by the long range interactions among ferroelectric domains composed of aligned P(VDF-TrFE-CTFE) dipoles. These interactions are realized through the compensation polarization outside the ferroelectric domain and are anisotropic in nature, when an external electric field is applied.[29] The relaxation properties of films with different crystal orientations were studied with the frequency spectra of *tan*δ, as shown in Fig. S4. All samples show only one relaxation peak at high frequencies (~ 1 MHz). The absence of relaxation peak at low frequency (~ 10 Hz) (α-relaxation) confirms the pure β crystals in all the films. After stretched, all films exhibit slightly reduced *tan*δ in the testing frequency range. Neither micro-Brownian motion of non-crystalline chain segments nor the molecular motion on the amorphous/crystalline interfaces in the stretched films is significantly altered comparing with the as-casted ones since the crystallinity is only slightly improved by the stretching as discussed above. In general, orienting the ferroelectric domains as well as the dipoles in amorphous phase by stretching the films uniaxially could effectively improve their ε_r but reduce their *tan*δ.

3.3 Evolution of D-E Loops under Elevated Electric Fields

It has been demonstrated that, upon polarization process under low electric field, the ferroelectric domains in PVDF based ferroelectrics could not orient to the direction of applied electric field because of the confine force around the domains and contribute little to the displacement. Upon depolarization process, the oriented dipoles characterized with a linear dielectric D-E loop. Polarizing the ferroelectric polymers under electric field over a critical field, the ferroelectric domains start to orient along the external field direction and contribute quickly improved displacement. Depending on the size and the polarity of the domains together with the confinement provided around them, the orientation and disorientation of ferroelectric domains take place under varied polarizing field and disorientation speed. First of all, the D-E loop would be fattened comparing with the skinny loop of linear dielectrics since the disorientation speed of ferroelectric domains is hindered due to the high coupling force between adjacent domains. Secondly, the confinement around the domains is crucial for the

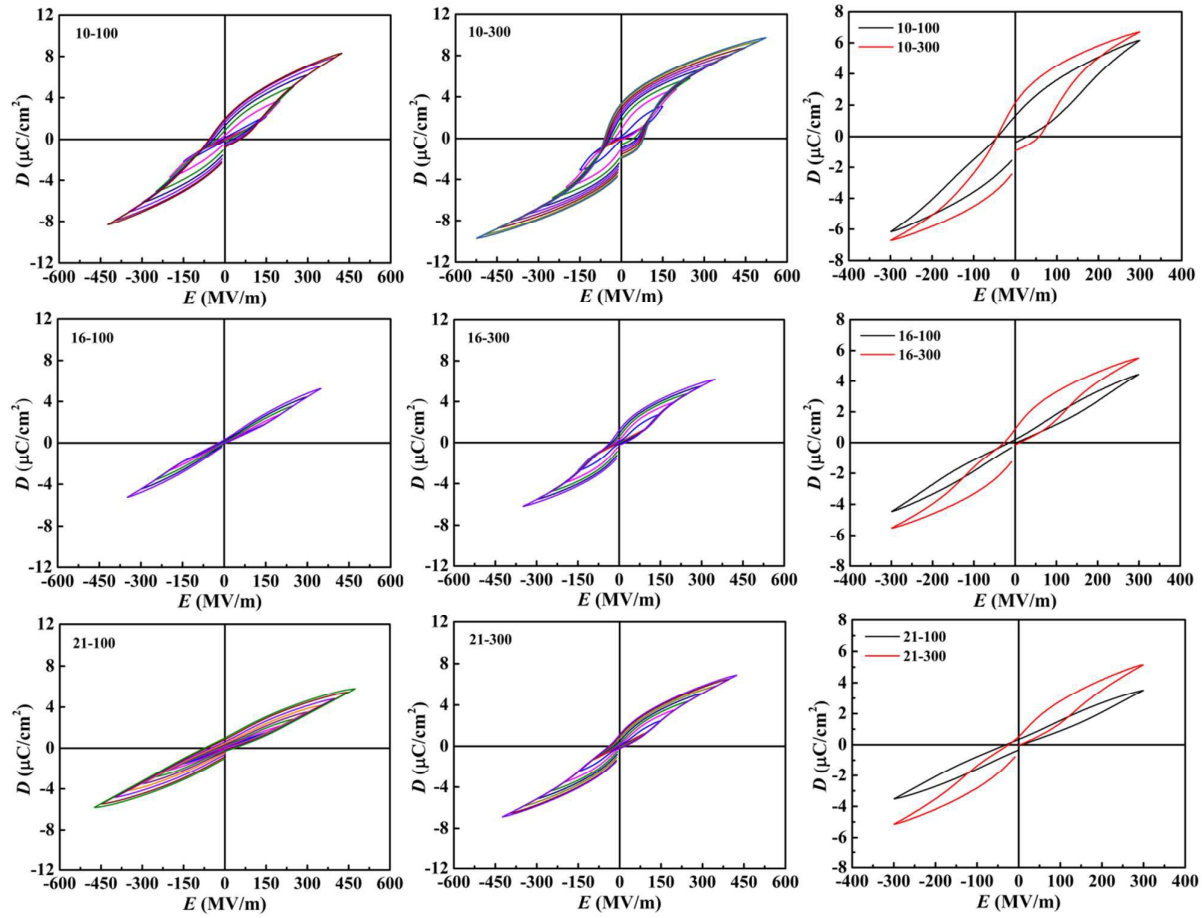

Fig. 5 Bipolar D-E loops of P(VDF-TrFE-CTFE)-*g*-PMMA films with varied PMMA contents before and after uniaxial stretching.

disorientation of these aligned domains. If the confinement is sufficient large, the domains would be disoriented mostly before the electric field reduced to zero and a rather low P_r would be observed at zero electric field. Then the profile is more like antiferroelectrics-like with a DHL profile. If the oriented domains could not be switched back to the random state before the electric field reduced to zero, an increased P_r would be obtained. As a result, the profile is more like relaxor or normal ferroelectrics. Apparently, the ferroelectric performance of the samples polarized under the elevated electric field may help to disclose the competition between the confinement around the ferroelectric grains and the ferroelectric phase characters. Therefore, it might be applied to characterize the phase transition happened in the materials induced by the stretching.

The dielectric properties of the P(VDF-TrFE-CTFE)-*g*-PMMA graft copolymer films with different degree of crystal orientation at high electric fields were studied with D-E hysteresis loop measurement as presented in Fig. 5. For the as-casted films, D-E loops of grafted polymers could be finely tuned by varying the PMMA content depending on the polarizing electric field. At lower PMMA content (c.a. 10 wt%), the grafted polymers exhibits D-E loops gradual evolution from linear dielectrics to anti-ferroelectric-like and relaxor ferroelectrics with the increasing of external electric field. As PMMA content increases to over 16 wt%, only evolution from linear dielectric to anti-ferroelectric-like performance would be observed even the poling field goes up to 400 MV/m. It has been well discussed that the D-E loops evolution is dominated by the confinement of rigid PMMA segments on the ferroelectric domains orientation and relaxation along the external field switching.[33] The confinement is in proportion to the content of PMMA, and the ferroelectric domains orientation is balanced by the confine force and the switching force constructed between the ferroelectric domains and the poling electric field.

For the sample 10-100 with lower content of PMMA, there were propeller-shaped D-E loops with two-step dipole switching depending on the external field. When the polarization field was less than 150 MV/m, it showed the linear dielectric performance with a narrow loop. Under electric field over 150 MV/m, relaxor ferroelectric or typical ferroelectric loops would be detected. Under electric field over 200 MV/m, relaxor and normal ferroelectric loops were obtained. Comparing with the relatively low critical electric field of 50-75 MV/m reported in P(VDF-TrFE) (VDF/TrFE = 80/20 mol%),[44] the introduction of rigid PMMA segments leads to improved critical field for the orientation of ferroelectric domains. However, the confinement contributed by the relatively low PMMA content is so poor that the DHL behavior of sample 10-100 could only be retained up to 200 MV/m. As PMMA content increases, the linear dielectric loops could be retained up to 300 MV/m in 24-100 sample. Over these critical fields, only antiferroelectric-like behavior with DHLs and no transition from antiferroelectric-like to relaxor or normal ferroelectric could be detected. That could be attributed to the continuously increased confinement effect of PMMA side chains and the gradually decreased ferroelectric domains.

After stretched for 300%, the linear dielectric loops could only bemaintained below 100 MV/m in all the samples. As external electric field increases, sample 10-300 is turned into relaxor and normal ferroelectric at about 200 MV/m, and the other stretched samples could retain the DHLs up to their breakdown (from 500 to 675 MV/m). No visible transition from antiferroelectriclike to relaxor or normal ferroelectric is observed, which is different from the previous report about the P(VDF-TrFE-CTFE)-g-PS copolymer.[30]

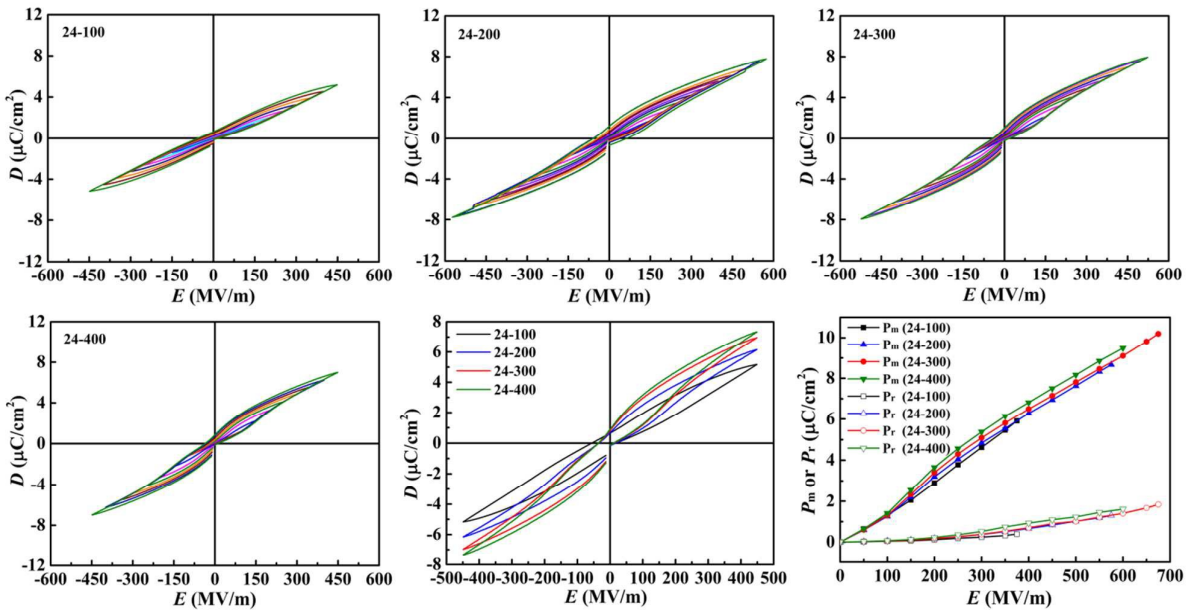

Fig. 6 Bipolar D-E loops, maximum polarization (P_m) and remnant polarization (P_r) as a function of electric field for P(VDF-TrFE-CTFE)-*g*-PMMA (24%) graft copolymer with different drawing ratio.

That means the balance between the confinement of the amorphous phase on the ferroelectric domains and the alignment force has been altered. Based on the DSC and XRD results discussed above, the improved ferroelectric domains and the crystallinity would lead to the elevated alignment force under the consistent external field. On the other hand, the uniaxial stretching induced molecular chain c-axe aligning along the direction is favorable for the flipping of the dipole moment along the electric field, which is responsible for the increased displacement under consistent electric field as well. These factors are responsible for the fattened loops and lowered critical field for retaining the linear dielectric behavior.

Both the fine confinement of aligned PMMA on P(VDF-TrFE-CTFE) and the dependence of phase transition evolution on the stretching ratios could be further confirmed by the polymers containing 24 wt% PMMA stretched with increased ratios. As indicated in Fig. 6, as stretching ratio increases, P_m is increasing gradually under the electric field over 100 MV/m while P_r shows little improvement. That is rather different from the results observed in P(VDF-TrFE-CTFE)-*g*-PS copolymers, where the P_r starts to increase significantly at 100 MV/m for the non-confinement of PS segments.[30] That could further confirm the conclusion that PMMA with fine compatibility with P(VDF-TrFE-CTFE) main chain and exhibit excellent confinement efficiency onto the disorientation of the aligned ferroelectric domains. In general, the desirable confinement of PMMA segments is allowing the orientation of the enlarged ferroelectric domains but forcing them back as soon as the electric field is removed.

3.4 Effect of stretching on the breakdown electric field

To examine how the stretching influences the breaking down quality of the films, E_b of polymer films were tested in various spots, and the experimental results were evaluated by the two-parameter Weibull analysis,[45,46] as illustrated by the following equation:

$$\mathbf{F(x) = 1 - \exp\left[-\left(\frac{x}{\alpha}\right)^{\beta}\right]}$$

wherein *x* is the measured E_b, scale parameter α is the field strength for which there is a 63.2% probability for the sample to breakdown (Weibull breakdown strength), and shape parameter β evaluates the scatter of data and a higher value of β represents higher level of dielectric reliability.

The characteristic E_b of the P(VDF-TrFE-CTFE)-*g*-PMMA copolymers with different contents of PMMA was analyzed with Weibull statistics and the results are presented in Fig. 7. For the as-casted films, E_b is enhanced from 249 MV/m (Fig. S3) for the solution-cast pristine P(VDF-TrFE-CTFE) to 310 MV/m for the grafted Discharged energy density (U_e) as a function of electric field copolymer with 24 wt% PMMA (24-100). In addition, the sample 24-100 also exhibited a relative narrow breakdown distribution with higher β of 10.1 than that for P(VDF-TrFE-CTFE) of 6.4 (Fig. S3) and indicated relatively higher level of dielectric reliability. Compared with E_b and β of P(VDF-TrFE-CTFE)-*g*-PMMA films with different PMMA content before and after uniaxial stretching, both E_b and β had been enhanced after stretching. With the same extension ratio, the films bearing higher PMMA content possess gradually elevated E_b from 342 MV/m in sample 10-300, to 478 MV/m of sample 24-300.

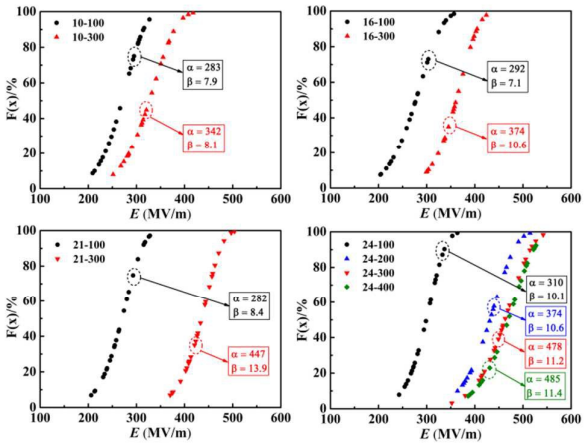

Fig. 7 Weibull distribution of the breakdown electric field for P(VDF-TrFE-CTFE)-*g*-PMMA films with varied PMMA contents before and after uniaxial stretching.

Meanwhile, E_b is gradually increased with the increasing of stretch ratio from the result of 24-100, 24-200, 24-300 and 24-400 samples.

Fundamentally, the enhanced E_b may be originated from the control of thin film morphology (including chain and/or crystal motion) under high applied electric fields. The local chain and/or polar crystal motions in the polymer thin films, which are essential for PVDF based ferroelectrics, may create free volume (or even defects) that are harmful to breakdown strength. As a result, the normal P(VDF-TrFE-CTFE) copolymers with crystals in large scale usually possess a low E_b near the polarization E_s, because the amorphous phase is more vulnerable to electrical breakdown after repeated flipping of large polar crystal domains. Introducing bulky commoners (such as CTFE and HFP),[4,47] chemically crosslinking PVDF or P(VDF-TrFE) followed by stretching or quenching films at extreme low temperature[48,49] could effectively reduce the crystal size and crystallinity, which may achieve high E_s as well as E_b in the resultant copolymers. Similarly, the incorporated PMMA would not only significantly decrease the crystal size and the crystallinity but also greatly improve E_s for the confinement effect. Therefore, by controlling the chain and crystal motion during the orientation polarization switching, the possible free volume (or even defects) formed would be greatly suppressed, and thus, substantially improved E_b is obtained in P(VDF-TrFE-CTFE)-*g*-PMMA copolymers. Most importantly, the defect inside the polymer film could reduce and subsequently the quality of film improved through stretching process, so the E_b had been further improved after uniaxial stretching.

3.5 Discharge Behaviors of Electric Energy Stored

It has been demonstrated that turning the normal ferroelectric behavior of P(VDF-TrFE)s into the anti-ferroelectric profiles in the grafted copolymers may successfully reduce the polarization under the consistent poling electric field and extend the polarization saturation field.[32,33] Thus, the films with improved quality are allowed to survive under high electric field, which benefits their energy storage capability. Meanwhile, uniaxial stretching in present

work could effectively enhance the uniformity and reduce the imperfects of the films. As a result, the breakdown strength and the stability under high electric field are improved as discussed above. The discharged electric energy storage density (U_e) was remarkablely improved as well as shown in Fig. 8, which were calculated from the unipolar D-E loops of different samples. For most of the samples, the stretching leads to the rather close U_e under the consistent electric field. The increasing of PMMA content results into the slightly increased U_e in the films stretched with same ratios under the consistent external field. However, the elevated E_b leads to significantly enhanced U_e, and the highest U_e of 23.3 J/cm^3 was obtained in the sample 24-300 under 675 MV/m field. But U_l under electric field between 100 and 300 MV/m is rather different. In the samples with lower content of PMMA (c.a. 10 wt%), U_l is slightly increased induced by the stretching. For the samples bearing more PMMA, U_l under this electric field range is significantly increased. It has been well discussed that U_l in this range is mostly originating from the relaxation of ferroelectric domains. At lower content, both the impedance and confinement PMMA onto the ferroelectric relaxation of as-casted films are rather poor and the relaxation induced U_l is high. After stretched, the films show only slightly increased crystallinity and ferroelectric domains. As a result, the ferroelectric relaxation of large scale ferroelectric domains induced U_l would be slightly improved as well. As PMMA content increases, both the impedance and confinement PMMA onto the ferroelectric relaxation of as-casted films are elevated, and the ferroelectric relaxation induced high U_l is quickly depressed in the as-casted films. However, the stretching leads to the significantly improved ferroelectric domains, crystallinity and the alignment of dipoles. All these factors are favorable for the increasing of ferroelectric relaxation induced U_l. Meanwhile, the increasing of PMMA would lead to the depressed ferroelectric relaxation as well as the reduced U_l in the stretched samples, which is very similar as that observed in the as-casted ones. When the electric field is over 500 MV/m as indicated in Fig. 8, U_l of the stretched samples is rather close to the as-casted one since most of the ferroelectric domains would be well oriented either in as-casted or stretched films and the displacement saturation is reached in both types of samples. The relatively low leakage current (< 10mA) under high electric field (1 kV to 10 kV) means that the resistance of the materials is about 10^7 Ω and the calculated electrical resistivity (ρ) is about 1.4-2.8 × 10^{12} Ω/m from the following formula, $\rho = R \times S/d$, where R is the resistance of the tested films (~10^7 Ω), S is the area of the samples (0.28 cm^2), and d is referring to the thickness of the films (10-20 μm). Although it is lower than that of BOPP (~ 10^{14} Ω/m), the extremely high energy storage capability is still attractive in high pulse discharged capacitors application, where the frequency of charging and discharging circle is not very high and the electrical energy is not necessarily stored over a long period.

4. Conclusions

In summary, the influence of uniaxial stretching on the crystalline, ferroelectric, dielectric and energy storage properties of P(VDF-TrFE-CTFE) grafted with varied content of PMMA side chains has been systematically presented. The uniaxial drawing leads to enhancement of both the size and content of crystalline and ferroelectric phase as well as the alignment of PMMA side chain in amorphous phase along the drawing direction. Thanks to the improved ferroelectric performance by stretching and the strong confinement of PMMA segments, the antiferroelectric-like behavior characterized with DHLs could be well retained in P(VDF-TrFE-CTFE)-*g*-PMMA under very high electric field (c.a. 675MV/m). That is responsible for the high discharged energy density of 23.3 J/cm^3 and relatively low energy loss of 29% obtained in P(VDF-TrFE-CTFE)-*g*-PMMA(24 wt%) sample with a 300% drawing ratio. Besides, the uniaxial drawing results into the significantly improved breakdown strength thus the dramatically enhanced serving reliability and the discharged energy density of the dielectric films. The results may help deeply understand how to tune the ferroelectric transition of PVDF based ferroelectric polymers and fabricate novel dielectric films for high pulse energy storage capacitors.

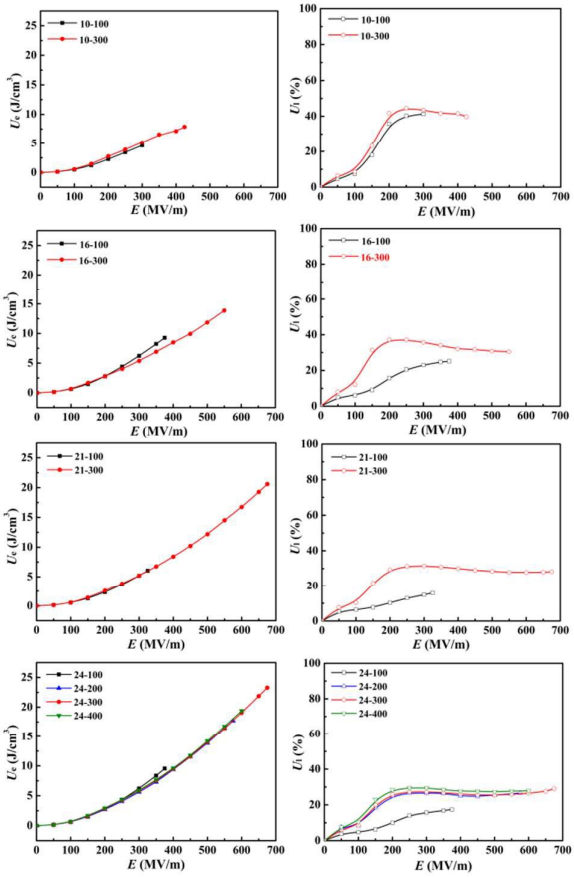

Fig. 8 Discharged energy density (U_e) as a function of electric field for the P(VDF-TrFE-CTFE)-*g*-PMMA graft copolymers with varied PMMA contents.

Acknowledgements

This work was financially supported by the National Nature Science Foundation of China-NSFC (No. 51573146, 51103115, 50903065), Fundamental Research Funds for the Central Universities (xjj2013075), the National Basic Research Program of China (No. 2009CB623306), International Science & Technology Cooperation Program of China (2013DFR50470), Natural Science Basic Research Plan in Shaanxi Province of China (No. 2013JZ003).

Notes and references

1 W. J. Sarjeant, *IEEE Trans. Electr. Insul.*, 1990, **25**, 861.
2 W. J. Sarjeant, J. Zirnheld and F. W. MacDougall, *IEEE Trans. Plasm. Sci.*, 1998, **26**, 1368.
3 W. J. Sarjeant, I. W. Clelland and R. A. Price, *Proc. IEEE*, 2001, **89**, 846.
4 B. Chu, X. Zhou, K. Ren, B. Neese, M. Lin, Q. Wang, F. Bauer and Q. M. Zhang, *Science*, 2006, **313**, 334.
5 H. M. Banford, R. A. Fouracre, A. Faucitano, A. Buttafava and F. Martinotti, *IEEE Trans. Dielectr. Electr. Insul.*, 1996, **3**, 594.
6 P. Michalczyk and M. Bramoulle, *IEEE Trans. Mag.*, 2003, **39**, 362.
7 X. Yuan and T. C. M. Chung, *Appl. Phys. Lett.*, 2011, **98**, 062901.
8 X. Yuan, Y. Matsuyama and T. C. M. Chung, *Macromolecules*, 2010, **43**, 4011.
9 T. C. M. Chung, *Green Sustain. Chem.*, 2012, **02**, 29.
10 M. Misra, M. Agarwal, D. W. Sinkovits, S. K. Kumar, C. Wang, G. Pilania, R. Ramprasad, R. A. Weiss, X. Yuan and T. C. M. Chung, *Macromolecules*, 2014, **47**, 1122.
11 Y. Tajitsu, A. Chiba, T. Furukawa, M. Date and E. Fukada, *Appl. Phys. Lett.*, 1980, **36**, 286.
12 A. J. Lovinger, *Science*, 1983, **220**, 1115.
13 Q. M. Zhang, V. Bharti and X. Zhao, *Science*, 1998, **280**, 2101.
14 Y. Wang, X. Zhou, Q. Chen, B. J. Chu and Q. M. Zhang, *IEEE Trans. Dielectr. Electr. Insul.*, 2010, **17**, 1036.
15 L. Zhu and Q. Wang, *Macromolecules*, 2012, **45**, 2937.
16 Q. J. Meng, W. J. Li, Y. S. Zheng and Z. C. Zhang, *J. Appl. Polym. Sci.*, 2010, **116**, 2674.
17 H. Xu, Z. Y. Cheng, D. Olson, T. Mai, Q. M. Zhang and G. Kavarnos, *Appl.Phys. Lett.*, 2001, **78**, 2360.
18 T. C. M. Chung and A. Petchsuk, *Macromolecules*, 2002, **35**, 7678.
19 M. Rahimabady, L. Q. Xu, S. Arabnejad, K. Yao, L. Lu, V. P. W. Shim, K. G. Neoh, E. T. Kang, *Appl. Phys. Lett.* 2013, **103**, 262904.
20 Y. Lu, J. Claude, B. Neese, Q. Zhang and Q. Wang, *J. Am. Chem. Soc.*, 2006, **128**, 8120.
21 Z. C. Zhang and T. C. M. Chung, *Macromolecules*, 2007, **40**, 783.
22 Z. C. Zhang and T. C. M. Chung, *Macromolecules*, 2007, **40**, 9391.
23 X. Zhou, B. J. Chu, B. Neese, L. Minren and Q. M. Zhang, *IEEE Trans. Dielectr. Electr. Insul.*, 2007, **14**, 1133.
24 V. Ranjan, L. Yu, M. B. Nardelli and J. Bernholc, *Phys. Rev. Lett.*, 2007, **99**, 047801.
25 V. Ranjan, M. B. Nardelli and J. Bernholc, *Phys. Rev. Lett.*, 2012, **108,** 087802.
26 Z. C. Zhang, Q. J. Meng and T. C. M. Chung, *Polymer*, 2009, **50**, 707.
27 F. Guan, J. Pan, J. Wang, Q. Wang and L. Zhu, *Macromolecules*, 2010, **43**, 384.
28 M. Rahimabady, S. Chen, K. Yao, F. E. H. Tay, L. Lu, *Appl. Phys. Lett.* 2011, **99**, 142901.
29 F. Guan, L. Yang, J. Wang, B. Guan, K. Han, Q. Wang and L. Zhu, *Adv. Funct. Mater.*, 2011, **21**, 3176.
30 L. Yang, E. Allahyarov, F. Guan and L. Zhu, *Macromolecules*, 2013, **46**, 9698.
31 F. Guan, J. Wang, L. Yang, J. K. Tseng, K. Han, Q. Wang and L. Zhu, *Macromolecules*, 2011, **44**, 2190.
32 J. J. Li, X. Hu, G. X. Gao, S. J. Ding, H. Y. Li, L. J. Yang and Z. C. Zhang, *J. Mater. Chem. C*, 2013, **1**, 1111.
33 J. J. Li, S. B. Tan, S. J. Ding, H. Y. Li, L. J. Yang and Z. C. Zhang, *J. Mater. Chem.*, 2012, **22**, 23468.
34 J. Wu, J. M. Schultz, F. Yeh, B. S. Hsiao and B. Chu, *Macromolecules*, 2000, **33**, 1765.
35 P. Sajkiewicz, A. Wasiak and Z. Gocłowski, *Eur. Polym. J.*, 1999, **35**, 423.
36 V. Sencadas, R. Gregorio and S. Lanceros-Mendez, *J. Macromol. Sci. B*, 2009, **48**, 514.
37 M. V. Mhalgi, D. V. Khakhar and A. Misra, *Polym. Eng. Sci.*, 2007, **47**, 1992.
38 A. Salimi and A. A. Yousefi, *Polym. Test.*, 2003, **22**, 699.
39 F. Fang, M. Z. Zhang and J. F. Huang, *J. Polym. Sci. B: Polym. Phys.*, 2005, **43**, 3255.
40 C. Zhao, M. Guo, Y. Lu and Q. Wang, *Macromol. Symp.*, 2009, **279**, 52.
41 X. Li, X. Qian, S. G. Lu, J. Cheng, Z. Fang and Q. M. Zhang, *Appl. Phys. Lett.*, 2011, **99**, 052907.
42 Q. Zhang, W. Xia, Z. Zhu and Z. Zhang, *J. Appl. Polym. Sci.*, 2013, **127**, 3002.
43 F. Guan, J. Wang, J. Pan, Q. Wang and L. Zhu, *Macromolecules*, 2010, **43**, 6739.
44 F. Guan, Z. Yuan, E. W. Shu and L. Zhu, *Appl. Phys. Lett.*, 2009, **94**, 052907.
45 Q. Li, K. Han, M. R. Gadinski, G. Zhang and Q. Wang, *Adv. Mater.*, 2014, **26**, 6244.
46 J. J. Li, H. H. Gong, Q. Yang, Y. C. Xie, L. J. Yang and Z. C. Zhang, *Appl. Phys. Lett.*, 2014, **104**, 263901.
47 X. Zhou, X. Zhao, Z. Suo, C. Zou, J. Runt, S. Liu, S. Zhang and Q. M. Zhang, *Appl. Phys. Lett.*, 2009, **94**, 162901.
48 S. B. Tan, X. Hu, S. J. Ding, Z. C. Zhang, H. Y. Li and L. J. Yang, *J. Mater. Chem. A*, 2013, **1**, 10353.
49 W. M. Xia, Z. Xu, F. Wen, W. J. Li and Z. C. Zhang, *Appl. Phys. Lett.*, 2010, **97**, 222905.

High-field Antiferroelectric-like Behavior in Uniaxially Stretched Poly(vinylidene fluoride-trifluoroethylene-chlorotrifluoroethylene)-*grafted*-poly(methyl methacrylate) Films with High Energy Density

Honghong Gong[a], Bei Miao[a], Xiao Zhang[b], Junyong Lu[*b], Zhicheng Zhang[*a]

[a]*Department of Applied Chemistry, MOE Key Laboratory for Nonequilibrium Synthesis and Modulation of Condensed Matter, School of Science, Xi'an Jiaotong University, Xi'an, P. R. China, 710049*

[b]*National Key Laboratory of Science and Technology on Vessel Integrated Power System, Naval University of Engineering, Wuhan, P. R. China, 430034*

[*]Email: zhichengzhang@mail.xjtu.edu.cn jylu@xinhuanet.com

Graphical Abstract

The antiferroelectric-like behavior could be retained up to 675 MV/m with a discharged energy density of 23.3 J/cm^3 in the P(VDF-TrFE-CTFE)-*g*-PMMA copolymer bearing 24 wt% PMMA with an extension ratio of 300% because of the strong confinement of rigid PMMA segment onto the ferroelectric relaxation of P(VDF-TrFE-CTFE) main chain and the alignment induced high breakdown strength.